Chapter 5

Homogenization Heat Treatment to Reduce the Failure of Heat Resistant Steel Castings

Mohammad Hosein Bina

Additional information is available at the end of the chapter

http://dx.doi.org/10.5772/50312

1. Introduction

In this chapter, influence of the homogenization heat treatment on the failure of heat resistant steel castings is studied. First, the cast stainless steels and effective factors on the failure of these steels are described. One of the most important factors is sigma phase embrittlement which is studied, in detail. Finally, the effect of homogenization heat treatment on dissolution of carbides and reduction of sigma-phase and failure is discussed. The present chapter is a compilation of my experience in industry and other studies about fracture of continuous annealing furnace rollers, prepared for use by practitioners and researchers. The chapter may also be useful for graduate students, researching failure.

2. Classification and designation of cast stainless steels

Cast stainless steels are usually classified as either corrosion resistant steel castings (which are used in aqueous environments below 650°C) or heat resistant steel castings (which are suitable for service temperatures above 650 °C). Cast stainless steels are most often specified on the basis of chemical composition using the designation system of the High Alloy Product Group of the Steel Founders Society of America [1].

2.1. Corrosion resistant steel castings

The corrosion resistant steel castings are widely used in chemical processes and electricity equipment that need corrosion resistant in aqueous or liquid-vapor environments at the temperatures less than 315°C. The serviceability of cast corrosion-resistant steels depends greatly on the absence of carbon, and especially precipitated carbides, in the alloy microstructure. Therefore, cast corrosion-resistant alloys are generally low in carbon (usually lower than 0.20% and sometimes lower than 0.03%). All cast corrosion-resistant steels contain more than 11% chromium [1].

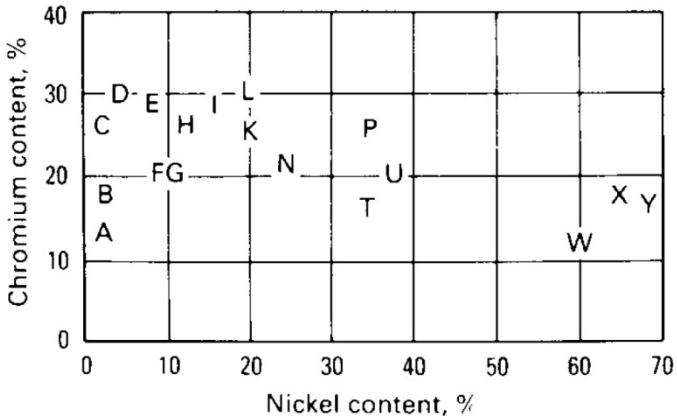

Figure 1. Chromium and nickel contents in ACI standard grades of heat- and corrosion-resistant steel castings [1].

2.2. Heat resistant steel castings

Stainless steel castings are classified as heat resistant if they are capable of sustained operation while exposed, either continuously or intermittently, to operating temperatures that result in metal temperatures in excess of 650°C. Heat resistant steel castings resemble high-alloy corrosion resistant steels except for their higher carbon content, which imparts greater strength at elevated temperature [1]. The three principal categories of H-type cast steels, based on composition, are [1–4]:

a. Iron-chromium alloys containing 10 to 30% Cr and little or no nickel. These alloys have low strength at elevated temperatures and are useful mainly due to their resistance to oxidation. Use of these alloys is restricted to conditions, either oxidizing or reducing, that involve low static loads and uniform heating. Chromium content depends on anticipated service temperature [1].
b. Iron-chromium-nickel alloys contain more than 13% Cr and 7% Ni (always more chromium than nickel) [1]. These austenitic alloys are ordinarily used under oxidizing or reducing conditions similar to those withstood by the ferritic iron-chromium alloys, but in service they have greater strength and ductility than the straight chromium alloys. They are used, therefore, to withstand greater loads and moderate changes in temperature. These alloys also are used in the presence of oxidizing and reducing gases that are high in sulfur content.
c. Iron-nickel-chromium alloys contain more than 25% Ni and more than 10% Cr (always more nickel than chromium) [1]. These austenitic alloys are used for withstanding reduction as well as oxidizing atmospheres, except where sulfur content is appreciable. (In atmospheres containing 0.05% or more hydrogen sulfide, for example, iron-chromium-nickel alloys are recommended [1].) In contrast with iron-chromium-nickel alloys, iron-nickel-chromium alloys do not carburize rapidly or become brittle and do not take up nitrogen in nitriding atmospheres. These characteristics become enhanced

as nickel content is increased, and in carburizing and nitriding atmospheres casting life increases with nickel content [1]. Austenitic iron-nickel-chromium alloys are used extensively under conditions of severe temperature fluctuations such as those encountered by fixtures used in quenching and by parts that are not heated uniformly or that are heated and cooled intermittently. In addition, these alloys have characteristics that make them suitable for electrical resistance heating elements.

3. Microstructure of heat resistant steels

The microstructure of a particular grade is primarily determined by composition. Chromium, molybdenum, and silicon promote the formation of ferrite (magnetic), while carbon, nickel, nitrogen, and manganese favor the formation of austenite (nonmagnetic). Chromium (a ferrite and martensite promoter), nickel, and carbon (austenite promoters) are particularly important in determining microstructure [1]. The heat resistant casting alloys (except HA-type) are contain high proportions of chromium and nickel that are generally austenitic and nonmagnetic. The austenite in the matrix provides useful high-temperature strength if it is adequately reinforced with particles of carbide and nitride. The austenite must contain no ferrite to reach maximum strength [5]. The microstructure of HH-type austenitic stainless steel castings (25Cr-12Ni) used in continuous annealing furnace rollers in un-worked condition is presented in Fig. 2. The ideal microstructure of HH alloy is

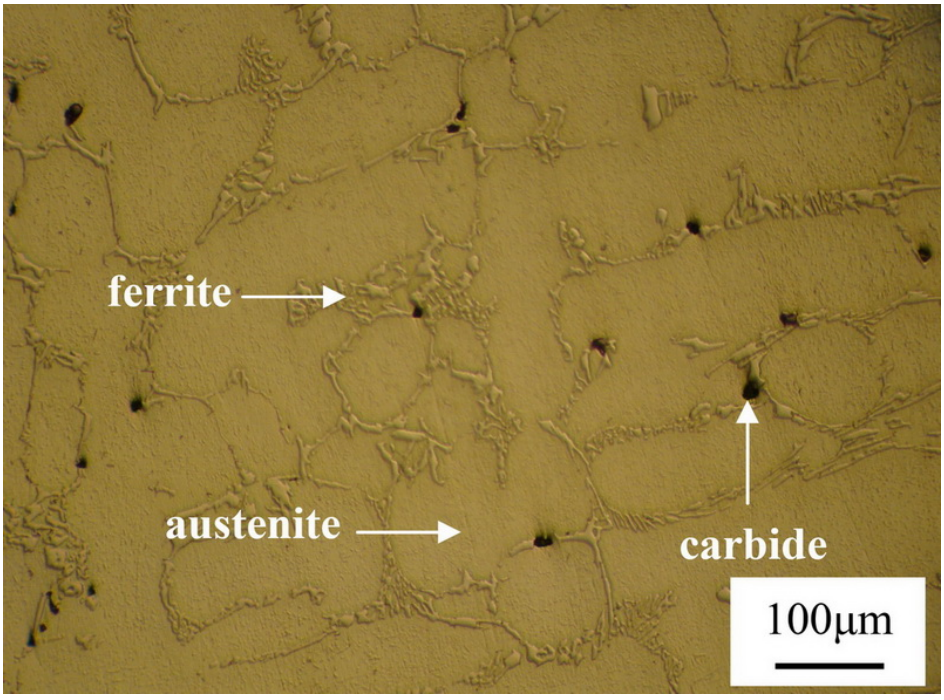

Figure 2. Microstructure of roller at un-worked condition (2% nital agent).

austenitic, while, in Fig. 2, the initial microstructure consisted of austenite, ferrite, and also black carbide particles. The presence of ferrite was attributed to un-controlled solidification and therefore, occurrence segregation phenomenon in the sample.

The presence of ferrite in microstructure may be beneficial or detrimental (especially at high temperatures), depending on the application. Ferrite can be beneficial in terms of weldability because fully austenitic stainless steels are susceptible to a weldability problem known as hot cracking, or microfissuring. But, at 540°C and above, the ferrite phase may transform to a complex iron-chromium-nickel-molybdenum intermetallic compound known as σ phase, which reduces toughness, corrosion resistance, and creep ductility [1]. The extent of the reduction in strength increases with time and temperature to about 815°C and may persist to 925°C [1].

4. Sigma phase embrittlement

Several factors cause failure of heat resistant steel castings such as oxidation, sulfidation, carburization, creep, thermal fatigue, and sigma phase embrittlement. Intermetallics such as the sigma phase are important sources of failure in high-temperature materials.

The existence of σ phase in iron-chromium alloys was first detected in 1907 by the observation of a thermal arrest in cooling curves [6]. The first actual observation of σ in iron-chromium alloys was reported in 1927 [7]. The σ phase was identified by x-ray diffraction in 1927 [8] and in 1931 [9]. After the existence of σ was firmly established, numerous studies were conducted to define the compositions and temperatures over which σ could be formed. In general, σ forms with long-time exposure in the range of 565 to 980°C, although this range varies somewhat with composition and processing [1]. Sigma phase has a tetragonal crystal structure with 30 atoms per unit cell and a *c/a* ratio of approximately 0.52 [10]. Sigma also forms in austenitic alloys. In fully austenitic alloys, σ forms from the austenite along grain boundaries. If δ-ferrite is present in the austenitic alloy, σ formation is more rapid and occurs in the δ-ferrite [1].

This phase is a unique combination of iron and chromium that produces a hard and brittle second phase. The presence of sigma phase not only results in harmful influence on the mechanical properties of the material, but also reduces its corrosion resistance by removing chromium and molybdenum from the austenitic matrix. A relatively small amount of sigma phase, when it is nearly continuous at a grain boundary, can lead to the very early failure of parts [11]. Fig. 3(a) shows a failed roller (HH-type) which was used for metal strip transfer in continuous annealing furnaces. An austenitic matrix and a network of sigma phase precipitates on austenitic grain boundaries in the failed roller is shown in Fig. 3(b). Formation of the sigma phase during prolonged heating at temperatures exceeding 650°C, results in a detrimental decrease in roller toughness at lower temperatures and during shut-down periods. Therefore, during shut-down, straightening or heating-up periods, the crack propagation along sigma phase at grain boundaries result in failure of rollers [12,13].

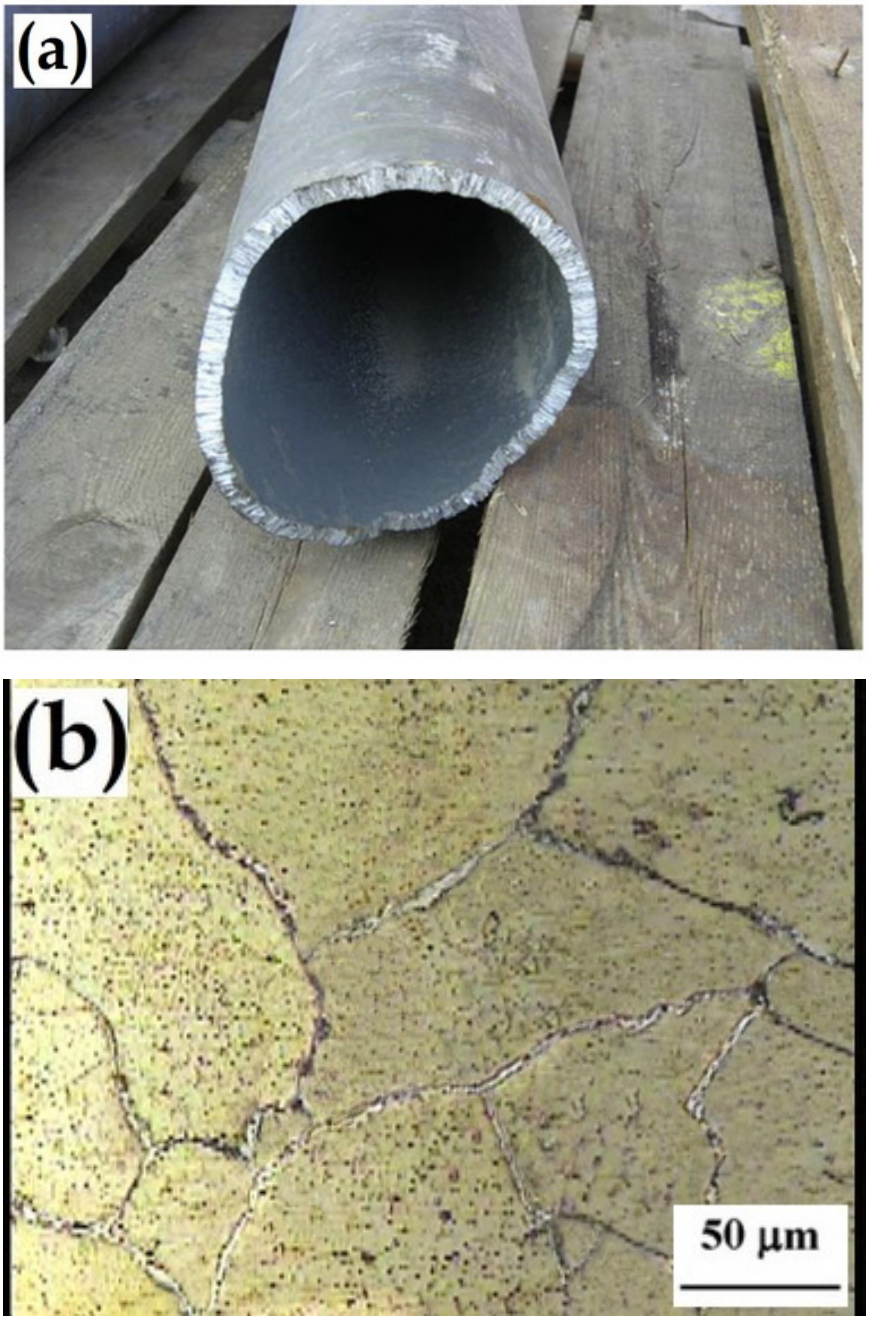

Figure 3. (a) View of the failed furnace roller, (b) microstructure of austenitic matrix and network of sigma phase precipitation on grain boundary (electrolytic etching) [13].

All of the ferritic stabilizing elements promote σ formation [1]. In commercial alloys, silicon, even in small amounts, markedly accelerates the formation of σ. In general, all of the elements that stabilize ferrite promote σ formation. Molybdenum has an effect similar to that of silicon, while aluminum has a lesser influence. Increasing the chromium content, also favors σ formation. Small amounts of nickel and manganese increase the rate of σ formation, although large amounts, which stabilize austenite, retard σ formation. Carbon additions decrease σ formation by forming chromium carbides, thereby reducing the amount of chromium in solid solution [14,15]. Additions of tungsten, vanadium, titanium, and niobium also promote σ formation. As might be expected, σ forms more readily in ferritic than in austenitic stainless steels [14–17].

4.1. Formation mechanism of sigma phase in heat resistant steels

Fig. 4 shows the formation mechanism of sigma phase in the failed roller. The presence of delta-ferrite in the austenitic matrix leads to accelerated sigma-phase formation. Generally, this phase nucleates inside delta-ferrite. Transformation of delta-ferrite can be described by two eutectoid reactions [1]:

$$\delta \rightarrow M_{23}C_6 + \gamma_2 \tag{1}$$

$$\delta \rightarrow \sigma + \gamma_2 \tag{2}$$

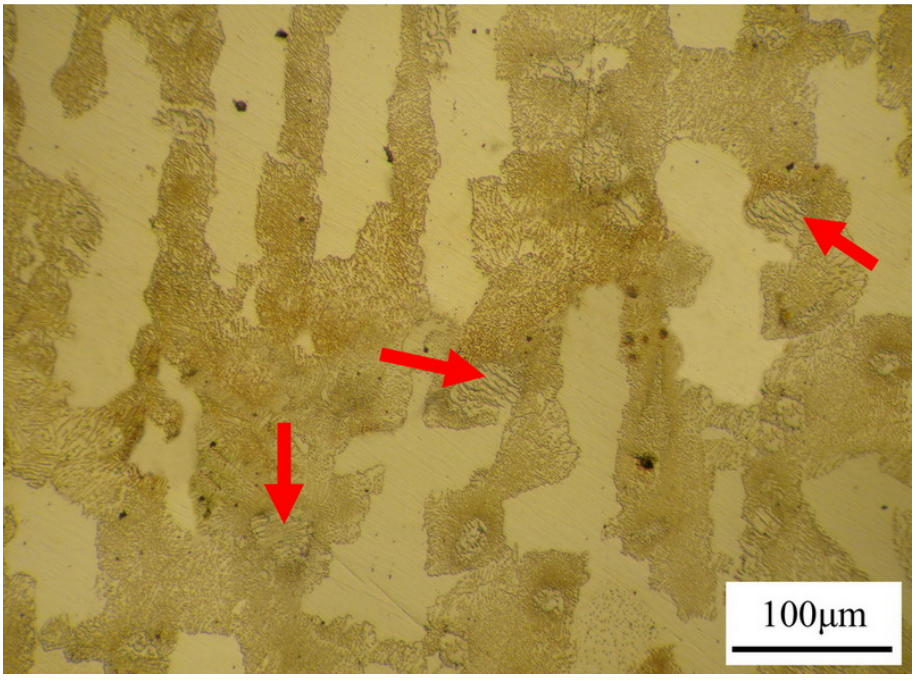

Figure 4. Formation of pearlite-like structure in the cross section of failed roller. The arrows show the large pearlite-like colonies.

By reaction (1), $M_{23}C_6$ carbides with lamellar morphology and also secondary austenite formed (Fig. 4). The mechanism of this reaction can be summarized as follows: first, the growth of carbide precipitates inside delta-ferrite lead to the formation of secondary austenite [18]. The chromium content near precipitates is high and results in increase in the content of chromium close to adjacent delta-ferrite. Therefore, the carbides growth develops inside delta-ferrite and a lamellar structure including carbides and secondary austenite is formed [19]. Finally, after completion of lamellar precipitation, the sigma-phase forms at foreside of the precipitates [19].

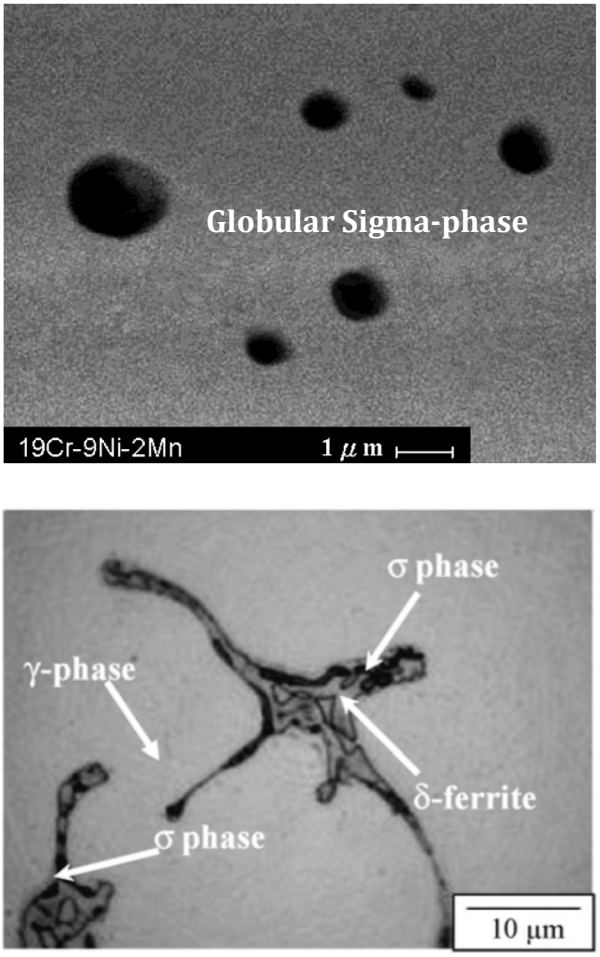

Figure 5. Various morphologies of sigma phase in a stainless steel [20].

4.2. Morphology of sigma phase

The morphologies of sigma-phase can be classified into dendritic and globular structures [17,20,21]. Fig. 5 shows the morphologies of sigma phase in a stainless steel (19Cr-9Ni-2Mn). The sigma-phase was formed by transformation of the delta-ferrite to the embrittling sigma-phase and secondary austenite due to unsuitable working conditions. Lin et al. [20] have pointed out that the dendrite-like sigma-phase is unstable, while the globular sigma-phase is a stable one. Furthermore, dendrite-like σ morphology was observed surrounding the δ-ferrite particles, which meant that the δ→σ phase transformation occurred partially [20]. Gill et al. [21] also have proposed that the spheroid σ phase results from the instability of dendritic sigma-phase to any localized decrease in width.

4.3. Precipitation sites of sigma phase

The precipitation sites of sigma-phase consist of δ/γ interface boundary, triple conjunction, grain corner and cellular which are shown in Fig. 6 [22]. The initial precipitation sites are δ/γ interphase boundary because it has higher boundary energy and many defects are concentrated here. Therefore, the precipitation of sigma-phase takes place preferentially at δ/γ boundary, and then precipitates toward interior of delta-ferrite grain [19,22]. The other precipitation sites were concentrated at δ-ferrite because σ-phase preferred to precipitate at a higher Cr content region [20,22]. The precipitation at grain corner meant that sigma-phase was strongly concentrated and formed at the corner of delta-ferrite. The precipitation at triple conjunction meant the σ-phase precipitated surrounding δ-ferrite. The cellular shape precipitation presented the eutectoid decomposition from delta-ferrite into sigma and secondary austenite phases that can be observed clearly at 800°C [22].

4.4. Effect of sigma phase on mechanical properties

One of the most affected mechanical properties of steels by formation of the sigma phase is impact energy. Effect of sigma phase on the impact energy of austenitic steel Fe-25Cr-20Ni is shown in Fig. 8 [23]. By increasing the time of exposure at formation temperature range of sigma phase (760–870°C), toughness value decreases by 85%.

The influence of high-temperature exposure on the toughness of a low-interstitial 29Cr-4Mo ferritic stainless steel has been examined (Fig. 9) by Aggen et al. [24]. In this figure, the C-curve shows the time for embrittlement as a function of aging temperature. For σ formation, embrittlement was most rapid at about 775°C, whereas 475°C embrittlement was slower with a maximum rate at about 480°C. In general, for this alloy, the sigma-phase forms over the range of 595 to 925°C. Embrittlement is most pronounced when intergranular σ films form, resulting in intergranular tensile and impact fractures [1].

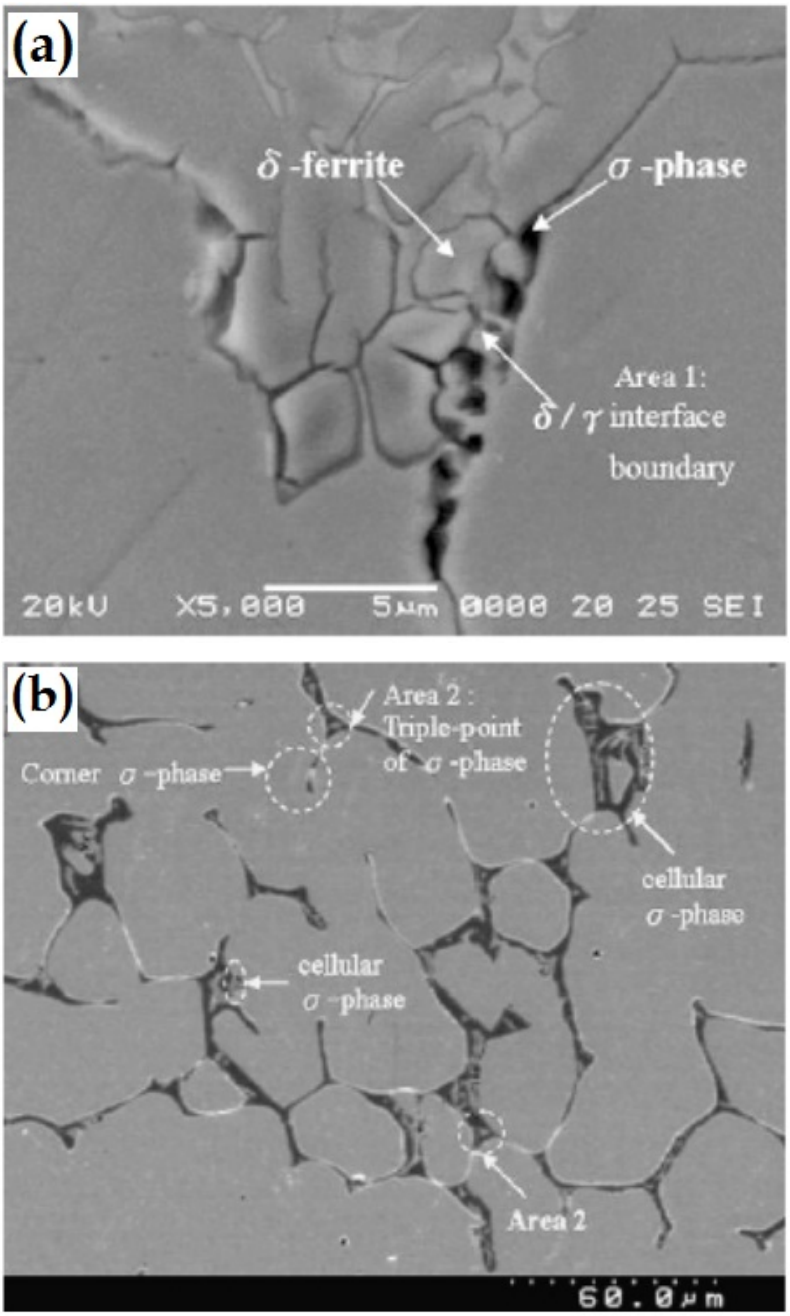

Figure 6. Precipitation of sigma-phase at: (a) δ/γ interface boundary, and (b) triple conjunction, grain corner and cellular [22].

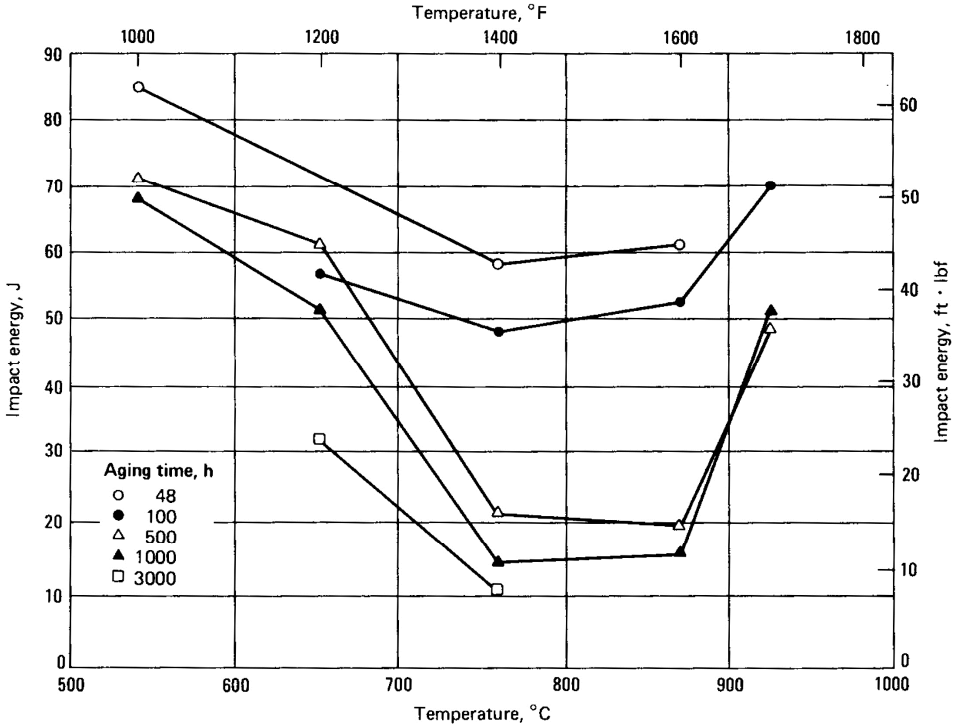

Figure 7. Effect of time and temperature of aging treatment on the impact energy of austenitic steel Fe-25Cr-20Ni [23].

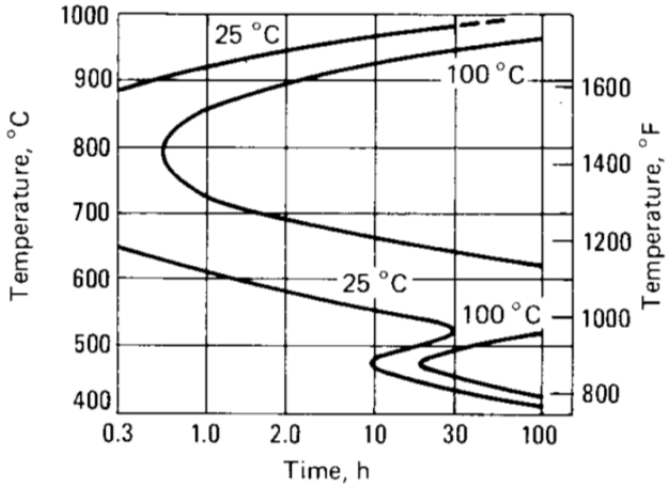

Figure 8. Time-temperature relationships to produce 25 and 100°C DBTTs for a 29Cr-4Mo ferritic stainless steel as a function of aging times that cover both the 475°C embrittlement range and the σ phase embrittlement range [24].

The hardness of sigma phase in Fe-Cr alloys is approximately 68 HRC [1]. Fig. 10 shows the microstructure of austenitic matrix and network of sigma phase precipitation on grain boundary and also indenter effects on the surface at several locations. It can be seen that because of brittleness and higher hardness of sigma phase with respect to the austenite matrix, this phase often fractures during indentation.

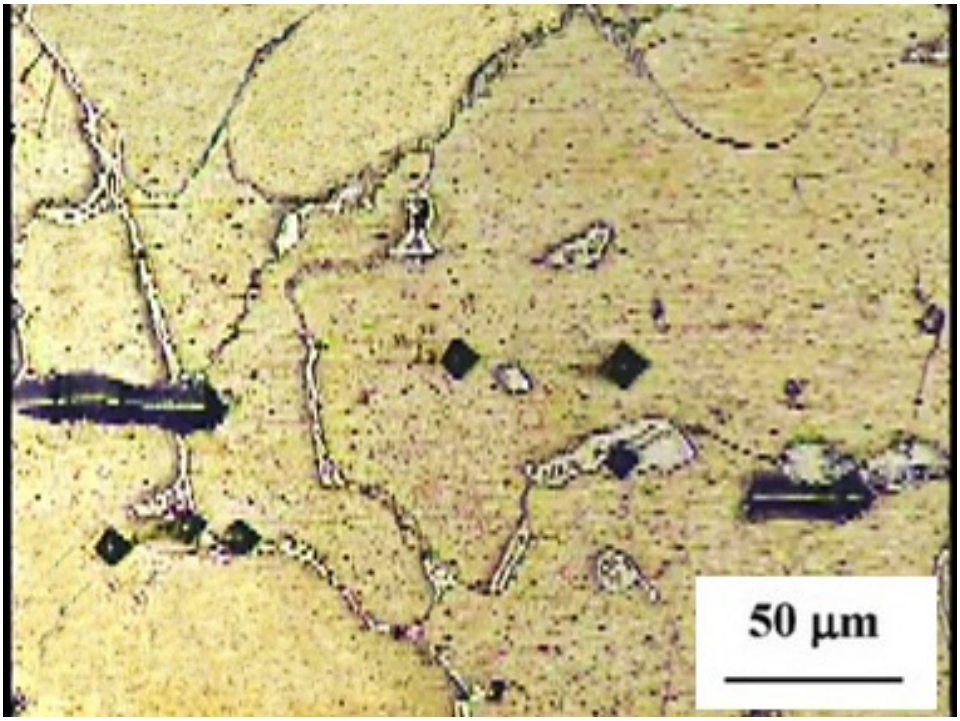

Figure 9. Microstructure of austenitic matrix and network of sigma phase precipitation on grain boundary. It can be seen that because of sigma is brittle phase, often fractures during indentation (indicated by the arrows) [12].

Therefore, a relatively small quantity of the σ phase, when it is nearly continuous at a grain boundary, can lead to very early failure of high-temperature parts [12].

5. Homogenization heat treatment

To eliminate segregation in the cast structure, it is frequently necessary to homogenize the part before usage to promote uniformity of chemical composition and microstructure. This treatment can also be used for complete dissolution of carbides and brittle and deleterious phases like sigma which are formed at operating conditions. In this method, steel is heated for a long enough period of time in order to complete the dissolution of carbides, and then the cooling starts at an appropriate rate to avoid formation of deleterious phases [12].

Specimen	Homogenization temperature (°C)	Cooling environment	Microstructures (etched electrolytically by 10 M KOH solution)	Microstructures (etched by Marble's reagent)
HH1	-	-	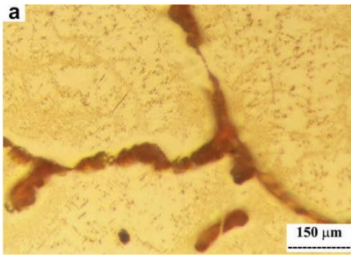	
HH2	950	Air	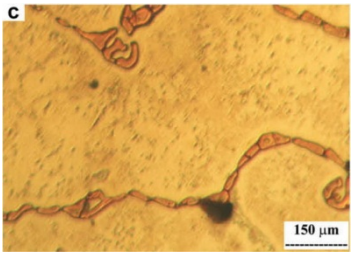	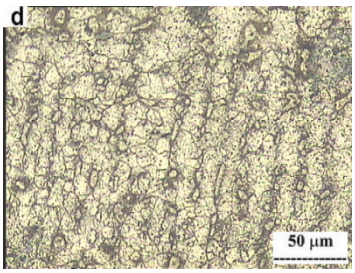
HH8	1050	Air	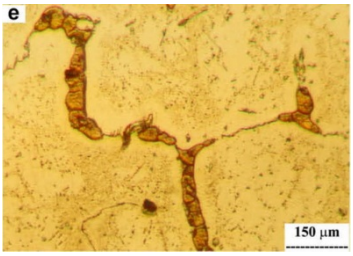	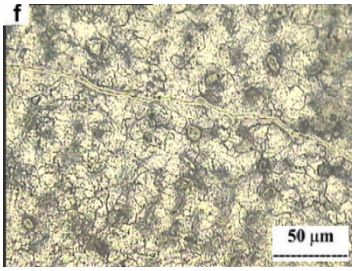
HH11	1100	Air		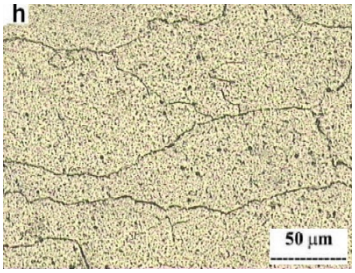

HH14	1100	Furnace		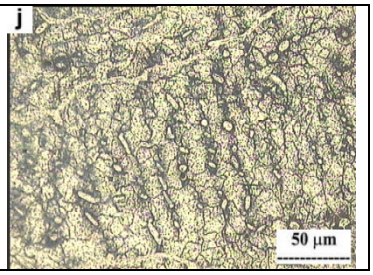

Table 1. Microstructures of selected failed roller steel, before and after the homogenization heat treatment for 2 h.

Microstructures of selected failed roller steel, before and after the homogenization heat treatment at various temperatures for 2 h are shown in Table 1. Formation of the brittle sigma phase and precipitation of carbides is clear in the microstructure of specimen HH14 when compared to the microstructure of specimen HH11. As a result of slow cooling in the furnace, all the desirable changes in the homogenized structure are reversed. In other words, the formation of carbide precipitates in grains, inhomogeneity of austenite as the matrix phase, and the formation of intermetallic brittle phases like sigma phase, which are all results of slow cooling at temperatures between 650 and 950°C, cause the toughness of the steel to decrease greatly. Since the formation of the sigma phase is a time consuming process, formation of this phase has been minimized by cooling in the air. The lowest amounts of sigma phase and carbides are in specimen HH11, which shows homogeneity of microstructure and a decrease in microscopic segregation. Therefore, for roller straightening and a good toughness to be obtained, homogenization heat treatment should be performed at 1100°C for at least 2 h followed by cooling in air [12].

Fig. 11 shows the precipitation sites of sigma-phase in the failed roller before and after the homogenization heat treatment at 1100 °C for 2 h followed by air cooling. Fig. 12 and Table 2 illustrate the chemical composition at three scanning points indicated in Fig. 11 (a), (b) and (c). As can be seen in Fig. 11, the points 1, 2, and 3 were austenite matrix, delta-ferrite, and sigma-phase, respectively. Table 2 shows that the chromium, molybdenum, and silicon content in the sigma-phase were higher than that of the austenite-phase. Generally, delta-ferrite and sigma-phase are Cr-rich. But, the weight percent of silicon and molybdenum in the delta-ferrite is higher than that of other phases (austenite and sigma). Silicon and molybdenum plays an important role in $\delta \rightarrow \sigma + \gamma_2$ phase transformation and acts as strong stabilizers for delta-ferrite [5,20].

As can be seen in Fig. 11, the heat treatment at 1100°C followed by cooling in air led to changing the morphology of sigma phase from dendritic structure (Figs. 11(a) and (b)) to globular structure (Fig. 11(c)). The dendritic sigma phase indicates an unstable shape, and globular sigma phase exhibits a stable shape. Also, the dendritic structure is brittle, while, the globular structure is ductile. Therefore, it can be concluded that for completing the transformation of delta-ferrite to sigma phase, the temperature of homogenization heat treatment should be increased to 1100°C and the morphology of sigma phase be

transformed to stable globular structure. This structure leads to remarkable increase in the impact energy and ductility of continuous annealing furnace roller. In contrast, the formation of sigma-phase with dendritic morphology results in decrease in ductility and failure of the roller.

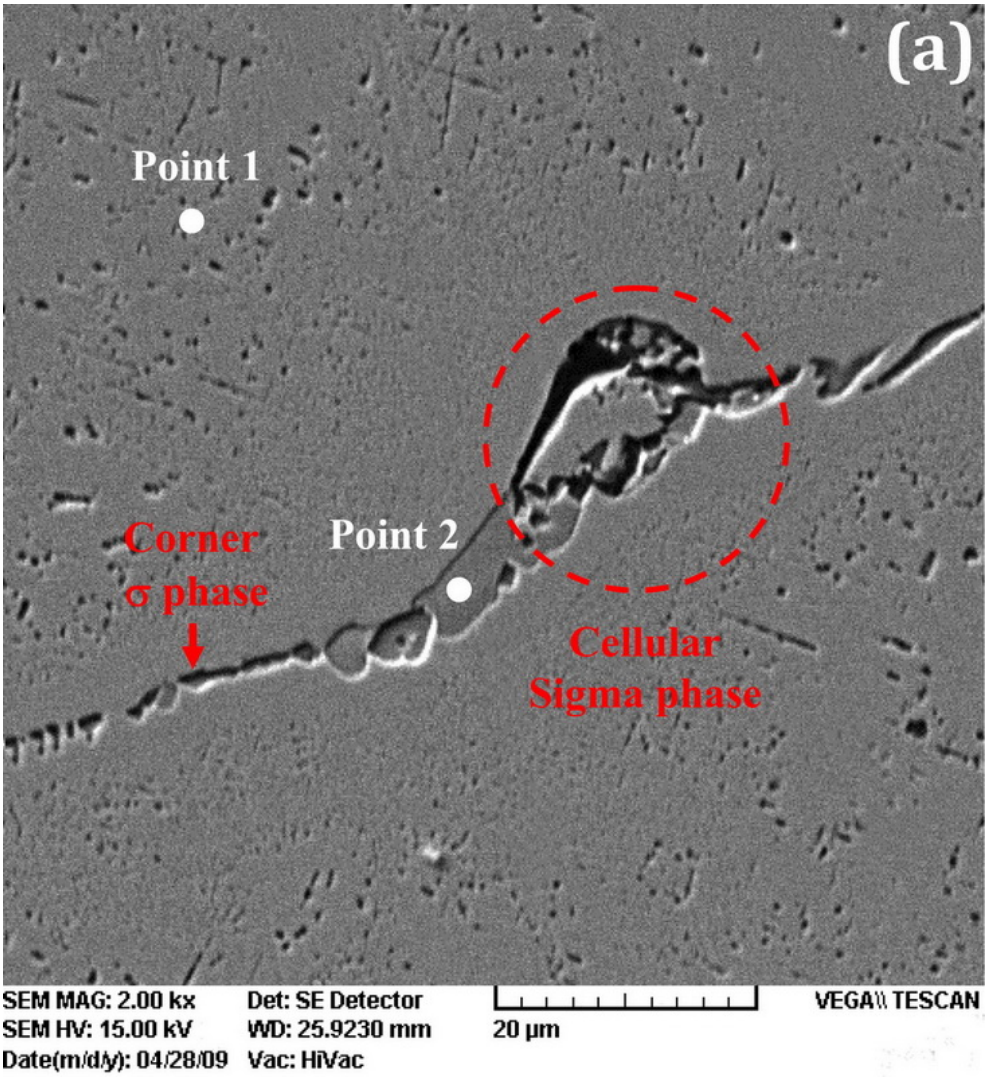

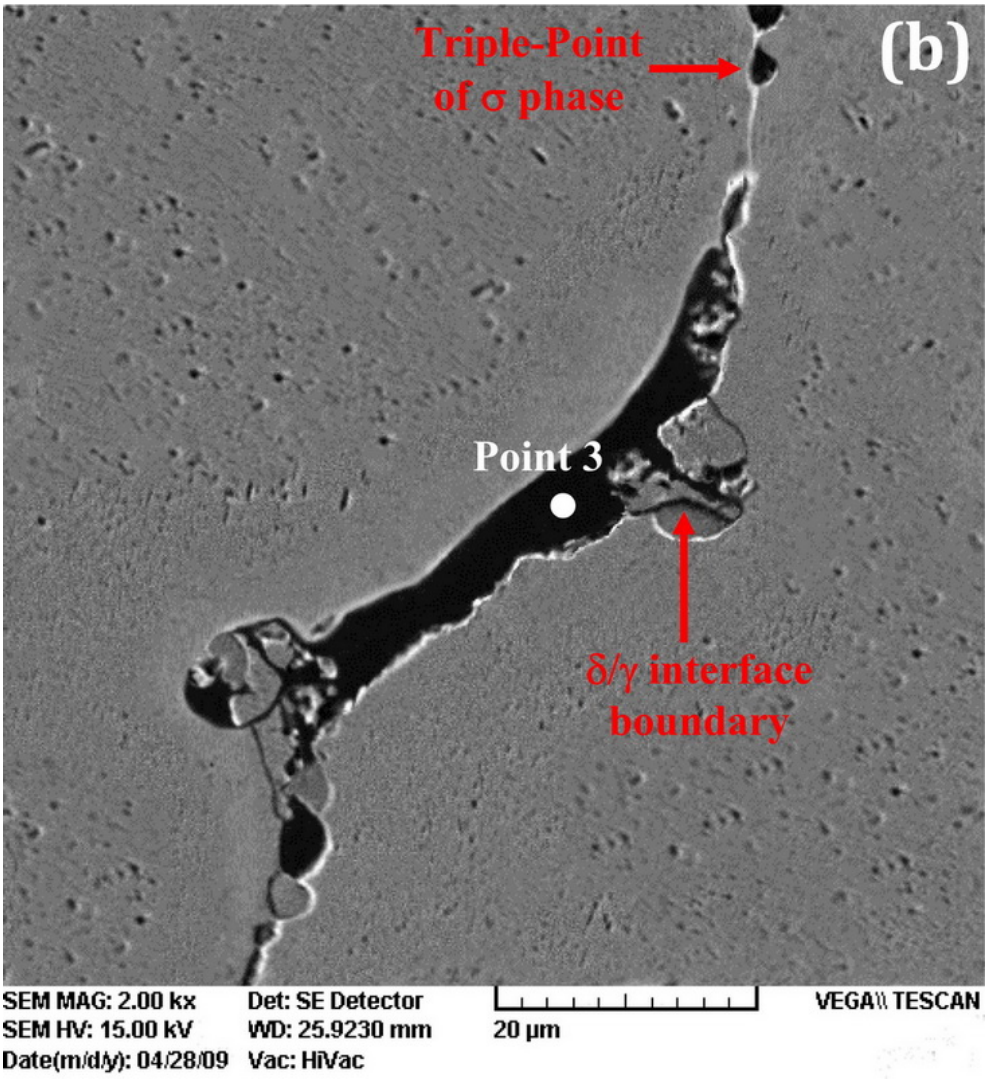
Triple-Point
of σ phase
(b)
Point 3
δ/γ interface
boundary
SEM MAG: 2.00 kx
SEM HV: 15.00 kV
Date(m/d/y): 04/28/09
Det: SE Detector
WD: 25.9230 mm
Vac: HiVac
20 µm
VEGA\\ TESCAN

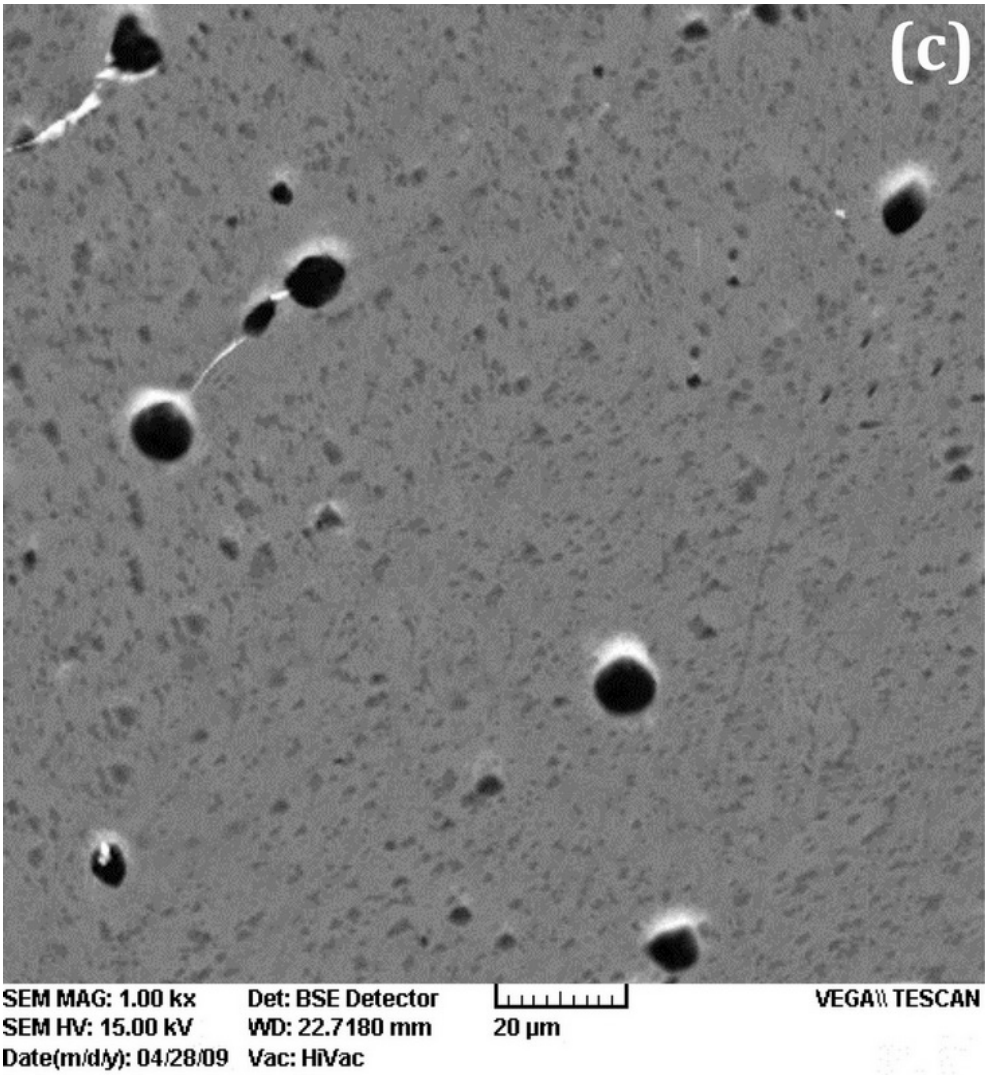

Figure 10. Morphology of sigma-phase. (a) and (b) after failure and before homogenization treatment, respectively and (c) after the homogenization heat treatment at 1100 °C for 2 h followed by air cooling.

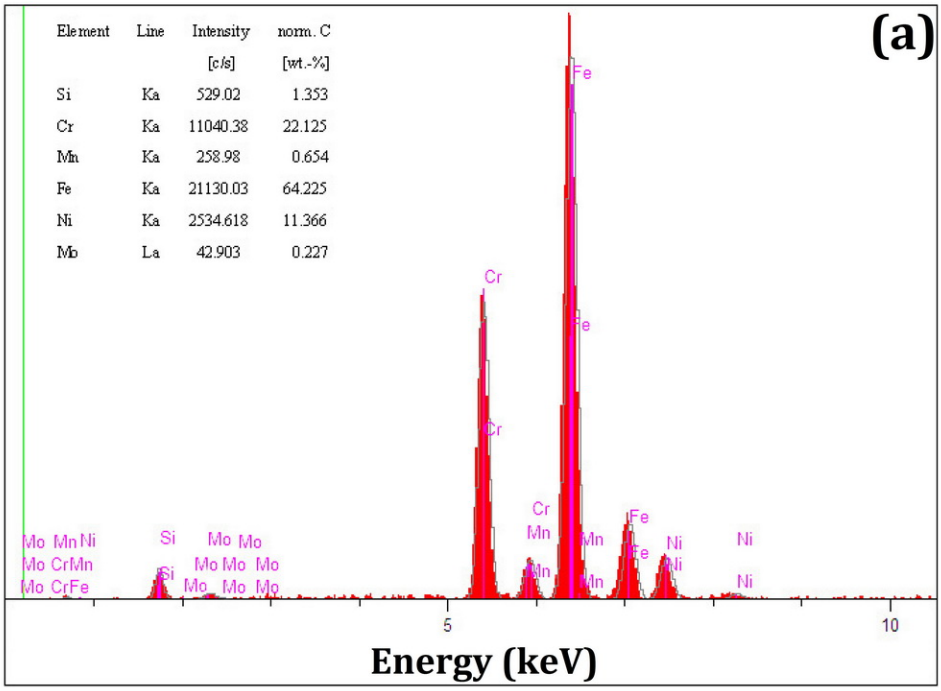
(a)
Element Line Intensity norm. C
[c/s] [wt.-%]
Si Ka 529.02 1.353
Cr Ka 11040.38 22.125
Mn Ka 258.98 0.654
Fe Ka 21130.03 64.225
Ni Ka 2534.618 11.366
Mo La 42.903 0.227
Energy (keV)

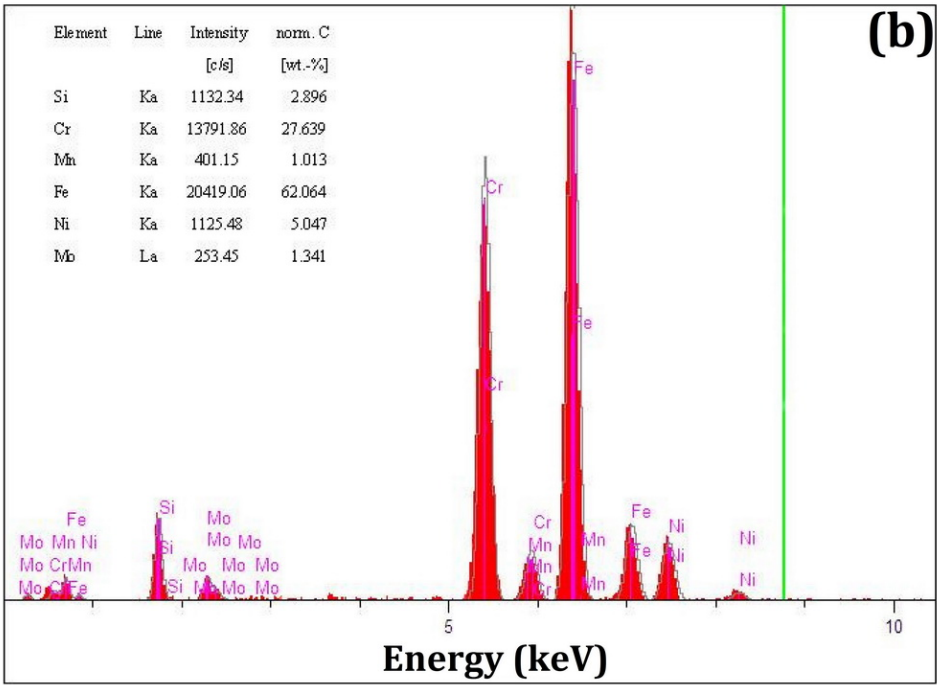
(b)
Element Line Intensity norm. C
[c/s] [wt.-%]
Si Ka 1132.34 2.896
Cr Ka 13791.86 27.639
Mn Ka 401.15 1.013
Fe Ka 20419.06 62.064
Ni Ka 1125.48 5.047
Mo La 253.45 1.341
Energy (keV)

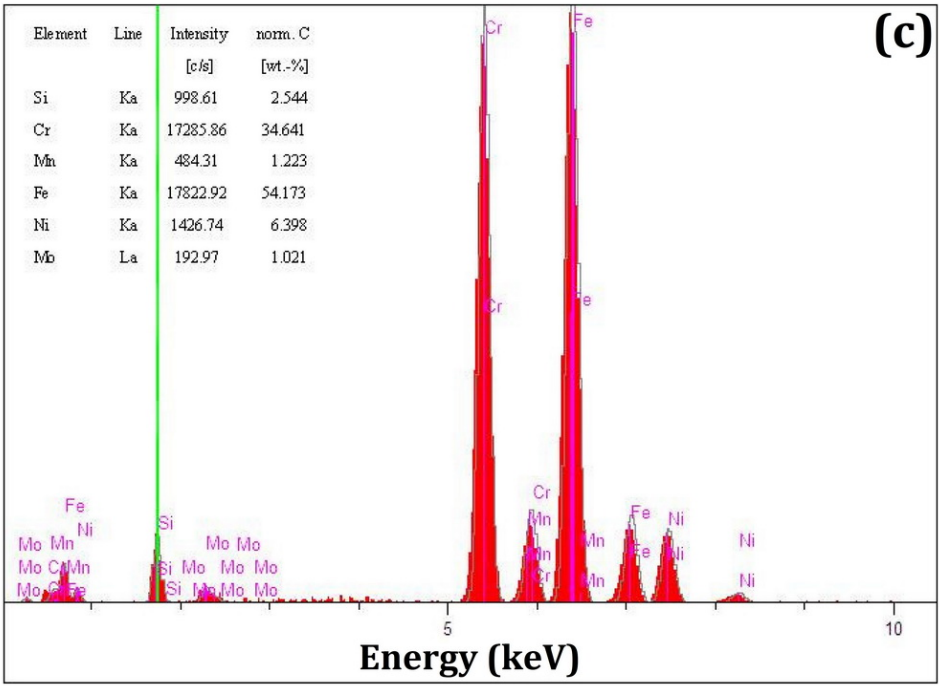

Figure 11. The EDS analysis of: (a) austenite-phase (point 1 in Fig. 11(a)), (b) ferrite-phase (point 2 in Fig. 11(b)), and (c) sigma-phase (point 3 in Fig. 11(c)).

Point	Element (wt.%)		
	Cr	Si	Mo
1 (gamma)	22.125	1.353	0.227
2 (delta)	27.639	2.896	1.341
3 (sigma)	34.641	2.544	1.021

Table 2. Elemental composition of Fig. 12.

Fig. 13 shows the fracture surfaces of the failed sample before homogenization (Fig. 13(a)), the sample after the homogenization heat treatment at 1100 °C for 2 h followed by cooling in furnace (Fig. 13(b)), and the sample after the homogenization heat treatment at 1100 °C for 2 h followed by cooling in air (Fig. 13(c)). The EDS analysis of points 1 and 2 in Figs. 13(a) and 13(b), respectively indicated the presence of sigma-phase in definite crystallographic planes. In fact, the fracture surface of failed sample (Fig. 13(a)) contained a random arrangement of flat surfaces and surfaces with steps which is characteristic of brittle fracture. The fracture surface of the sample after the homogenization heat treatment at 1100 °C for 2 h followed by cooling in furnace (Fig. 13(b)) was a mixture of small dimples and layered surfaces that indicated brittle and ductile fractures in this sample. The EDS analysis of point 3 in Fig. 13(b) showed the presence of chromium in the form of carbide particles. The carbide

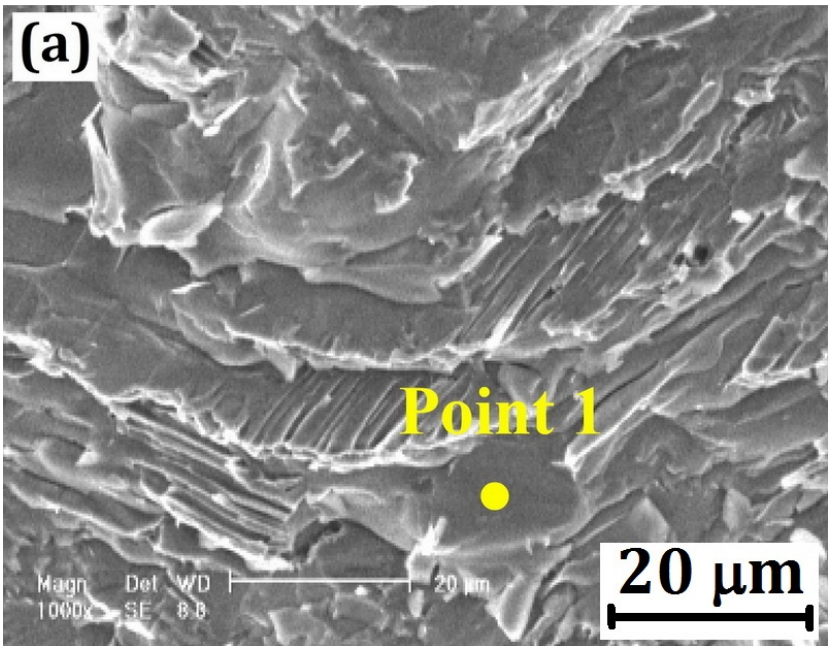
(a)
Point 1
Magn Det WD
1000x SE 8.8
20 µm
20 µm

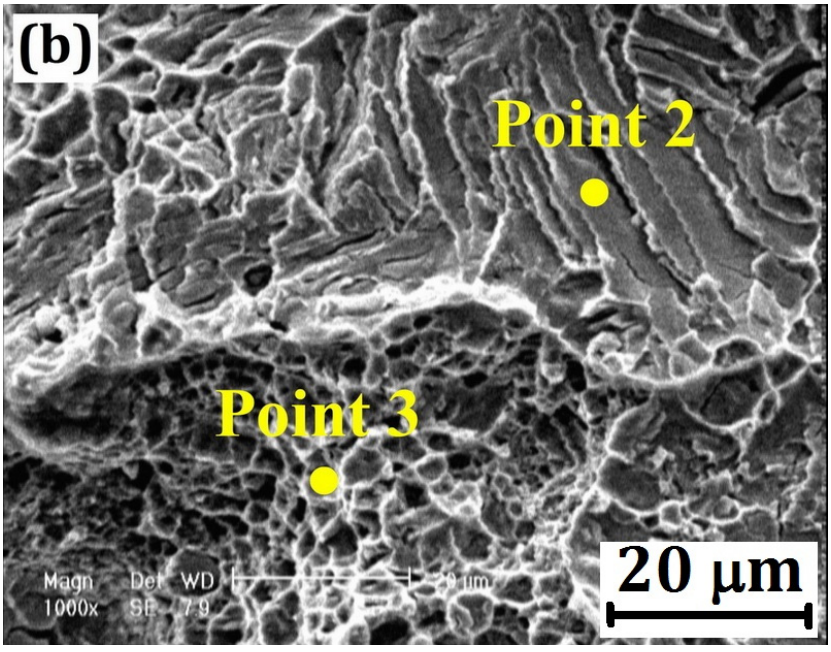
(b)
Point 2
Point 3
Magn Det WD
1000x SE 7.9
20 µm
20 µm

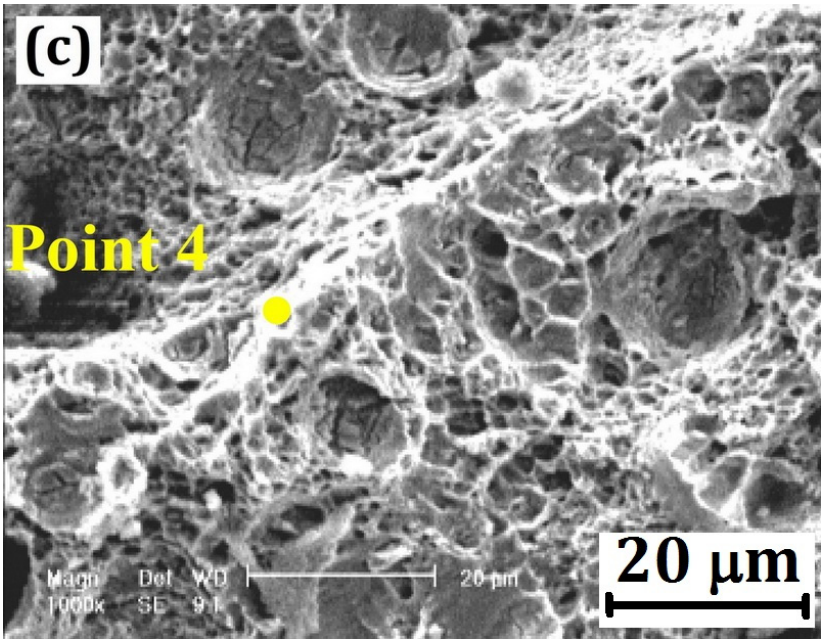

Figure 12. Fracture surfaces of: (a) the failed sample before homogenization, (b) the sample after the homogenization heat treatment at 1100 °C for 2 h followed by cooling in furnace, and (c) followed by cooling in air.

particles existed in the center of small dimples. According to EDS analysis of points 2 and 3, it can be said that due to slow cooling rate in the furnace, all the desirable changes that occur in homogenized structures are reversed and a new formation of the sigma-phase and precipitates in the sample results in a transition from ductile to almost brittle fracture. As can be seen in Fig. 13(c), formation of deep dimples is a main characteristic of ductile fracture. The EDS analysis of the point 4 was similar to the base metal. This figure indicated a considerable decrease in sigma phase and precipitates amounts after homogenization.

Therefore, before roller straightening, the homogenization heat treatment should be performed for dissolution of deleterious phases in austenite as the matrix phase and obtaining good toughness. In many cases, microstructural inhomogeneity can be eliminated by holding the sample at high temperatures for a sufficient time and cooling at an appropriate rate. Otherwise, the possibility of the formation of fine cracks during roller straightening is very high. These cracks can result in roller fracture during the straightening process and/or in the continuous-annealing furnace.

6. Conclusions

The sigma phase tends to precipitate in the regions of high chromium content, such as the chromium carbides in the grain. A relatively small quantity of the σ phase, when it is nearly

continuous at a grain boundary, can lead to very early failure of high-temperature parts. It is important to understand that the sigma-phase cannot undergo any significant plastic deformation; instead, it fractures even at relatively low strain levels. This is true at elevated temperatures, but even more so at ambient temperature. Where toughness and ductility are an important part of the system design, the sigma-phase cannot be tolerated. The formation of sigma-phase with dendritic morphology results in decrease in ductility and failure of heat resistant steels. The microstructural inhomogeneity (sigma-phase and carbides) can be eliminated by holding the sample at high temperatures for a sufficient time and cooling at an appropriate rate. The homogenization heat treatment under appropriate condition can led to change in the morphology of sigma phase from dendritic structure to globular structure. This structure leads to remarkable increase in the impact energy and ductility of heat resistant steels.

Author details

Mohammad Hosein Bina
Department of Advanced Materials and New Energy, Iranian Research Organization for Science and Technology, Tehran, Iran

7. References

[1] ASM Handbook, Volume 1, Properties and Selection: Irons, Steels, and High-Performance Alloys, ASM International, Materials Park, Ohio, 2005.
[2] Lamb, S., Practical Handbook of Stainless Steels and Nickel Alloys, ASM International, Materials Park, Ohio, 1999.
[3] ASM Handbook, Volume 15, Casting, ASM International, Materials Park, Ohio, 2005.
[4] Shi, S. and Lippold, J.C., "Microstructure Evolution During Service Exposure of Two Cast, Heat-Resisting Stainless Steels - Hp-Nb Modified and 20-32nb", Materials Characterization, Vol. 59, No. 8, pp. 1029–1040, 2008.
[5] Prager, M. and Svoboda, J., Cast High Alloy Mettalurgy, Steel Casting Metallurgy, Steel Founder's Society of America, Rocky River, OH, 1984.
[6] W. Trietschke and G. Tammnann, The Alloys of Iron and Chromium. Zh. Anorg. Chem., Vol 55, 1907, p 402–411.
[7] E.C. Bain and W.E. Griffiths, An Introduction to the Iron-Chromium-Nickel Alloys, Trans. AIME, Vol 75, 1927, p 166–213.
[8] P. Chevenard, Experimental Investigations of Iron, Nickel, and Chromium Alloys, Trav. Mem., Bur. Int. Poids et Mesures, Vol 17, 1927, p 90.
[9] F. Wever and W. Jellinghaus, The Two-Component System: Iron-Chromium, Mitt. Kaiser-Wilhelm Inst., Vol 13, 1931, p 143–147.
[10] E.O. Hall and S.H. Algie, The Sigma Phase, Metall. Rev., Vol 11, 1966, p 61–88.
[11] ASM Handbook, Volume 11, Failure Analysis and Prevention, ASM International, Materials Park, Ohio, 2002.

[12] Bina, M.H., Dini, G., Vaghefi, S.M.M., Saatchi, A., Raeissi, K. and Navabi, M., "Application of Homogenization Heat Treatments to Improve Continuous-Annealing Furnace Roller Fractures", Engineering Failure Analysis, Vol. 16, No. 5, pp. 1720–1726, 2009.

[13] Dini, G., Bina, M.H., Vaghefi, S.M.M., Raeissi, K., Safaei-Rad, M. and Navabi, M., "Failure of a Continuous-Annealing Furnace Roller at Mobarakeh Steel Company", Engineering Failure Analysis, Vol. 15, No. 7, pp. 856–862, 2008.

[14] A.J. Lena and W.E. Curry, The Effect of Cold Work and Recrystallization on the Formation of the Sigma Phase in Highly Stable Austenitic Stainless Steels, Trans. ASM, Vol 47, 1955, p 193–210.

[15] ASM Handbook, Volume 19, Fatigue and Fracture, ASM International, Materials Park, Ohio, 2005.

[16] ASM Handbook, Volume 12, Fractography, ASM International, Materials Park, Ohio, 2005.

[17] Lin, D.Y., Liu, G.L., Chang, T.C. and Hsieh, H.C., "Microstructure Development in 24Cr-14Ni-2Mn Stainless Steel after Aging under Various Nitrogen/Air Ratios", Journal of Alloys and Compounds, Vol. 377, No. 1-2, pp. 150-154, 2004.

[18] Tseng, C.C., Shen, Y., Thompson, S.W., Mataya, M.C. and Krauss, G., "Fracture and the Formation of Sigma Phase, M23C6, and Austenite from Delta-Ferrite in an AISI 304L Stainless Steel", Metallurgical and Materials Transactions A, Vol. 25, No. 6, pp. 1147–1158, 1994.

[19] Martins, M. and Casteletti, L.C., "Sigma Phase Morphologies in Cast and Aged Super Duplex Stainless Steel", Materials Characterization, Vol. 60, No. 8, pp. 792–795, 2009.

[20] Hsieh, C.C., Lin, D.Y. and Wu, W., "Precipitation Behavior of σ Phase in 19Cr-9Ni-2Mn and 18Cr-0.75Si Stainless Steels Hot-Rolled at 800 °C with Various Reduction Ratios", Materials Science and Engineering A, Vol. 467, No. 1-2, pp. 181–189, 2007.

[21] Gill, T.P.S., Vijayalkshmi, M., Rodriguez, P. and Padmanabhan, K.A., "On Microstructure-Property Correlation of Thermally Aged Type 316L Stainless Steel Weld Metal", Metallurgical Transactions A, Vol. 20, No. 6, pp. 1115–1124, 1989.

[22] Hsieh, C.C., Lin, D.Y. and Chang, T.C., "Microstructural Evolution During the $\delta/\sigma/\gamma$ Phase Transformation of the Sus 309L Si Stainless Steel after Aging under Various Nitrogen Atmospheric Ratios", Materials Science and Engineering A, Vol. 475, No. 1-2, pp. 128–135, 2008.

[23] G.N. Emanuel, Sigma Phase and Other Effects of Prolonged Heating at Elevated Temperatures on 25 Per Cent Chromium-20 Per Cent Nickel Steel, in Symposium on the Nature, Occurrence, and Effects of Sigma Phase, STP 110, American Society of Testing and Materials, 1951, p 82–99.

[24] G. Aggen et al., Microstructures Versus Properties of 29-4 Ferritic Stainless Steel, in MiCon 78: Optimization of Processing, Properties, and Service Performance Through Microstructural Control, STP 672, American Society for Testing and Materials, 1979, p 334–366.